Computational Fluid Dynamics-based Aero-servo-elastic Analysis for Gust Load Alleviation

Journal:	*Journal of Aircraft*
Manuscript ID	2017-06-C034621.R1
Manuscript Type:	Full Paper
Date Submitted by the Author:	21-Nov-2017
Complete List of Authors:	Chen, Gang; Xi'an Jiaotong University, School of Aerospace zhou, qiang; No. 38 Research Institute of China Electronics Technology Group Corporation Da Ronch, Andrea; University of Southampton LI, Yueming; Xi'an Jiaotong University, School of Aerospace
Subject Index Category:	00200 Aeroelasticity and Aeroservoelasticity < 00000 AIRCRAFT TECHNOLOGY, CONVENTIONAL, STOL/VTOL, 20500 Computational Fluid Dynamics < 20000 FLUID DYNAMICS

Computational Fluid Dynamics-based Aero-servo-elastic Analysis for Gust Load Alleviation

Gang Chen [1]
State Key Laboratory for Strength and Vibration of Mechanical Structures; Shaanxi Key Laboratory for Environment and Control for Flight Vehicle, Xi'an Jiaotong University, Xi'an, 710049, China

Qiang Zhou [2]
No.38 Research Institute of China Electronics Technology Group Corporation, Hefei, China

Andrea Da Ronch [3]
University of Southampton, Southampton, SO17 1BJ, U.K.

and
Yueming Li [4]
School of Aerospace, Xi'an Jiaotong University, Xi'an, China

Gust load alleviation using computational fluid dynamics as source of the aerodynamic predictions is carried out in the time domain. To this goal, an aero-servo-elastic reduced order model is generated. The model capitalises on two key aspects: a dimensional reduction through proper orthogonal decomposition, further enhanced via balanced truncation; and an analytically-derived mechanism to reproduce the gust effects in the reduced order model. The compact model in state-space form thus obtained was then used for control design synthesis. Assuming information on the structural motion only is accessible for feedback, a linear quadratic regular was designed, first, on the reduced model, and then validated on the large computational model. Results are presented for two configurations: an aerofoil and the modified AGARD

1. Professor, School of Aerospace, Email: aachengang@mail.xjtu.edu.cn (Corresponding Author)
2. Doctor, No.38 Research Institute of China Electronics Technology Group Corporation, Email: zhouqiang@stu.xjtu.edu.cn
3. New Frontiers Fellow & Lecturer, Faculty of Engineering and the Environment, AIAA Member. Email: A.Da-Ronch@soton.ac.uk
4. Professor, School of Aerospace, Email: liyueming@mail.xjtu.edu.cn

445.6 wing, both with a trailing-edge control surface. Studies are presented for the gust response to discrete gusts and continuous turbulence. In particular, for the latter, the standard deviation of the loads and the structural motion was reduced as much as 77%.

Nomenclature

a	=	speed of sound
$\mathbf{A}$	=	volume of fluid cell
b	=	reference semi-chords
c	=	parameter to be identified in the reduced model
C_L	=	lift coefficient
C_M	=	moment coefficient
u_g	=	gust moving velocity
ρ	=	freestream density
V	=	freestream speed
M	=	freestream Mach number
$\mathbf{F}$	=	inviscid flux value
t	=	fluid non-dimensional time
τ	=	structural dimensional time
q	=	The dynamic pressure, $q = 1/2\,\rho \mathrm{V}^2$.
w_g	=	gust velocity
w_{g0}	=	the magnitude of sharp-edge gust
λ	=	advance ratio
α	=	angle of attack
δ	=	control surface deflection
$\mathbf{w}$	=	conservative flow variable
$\mathbf{f}^{\mathrm{ext}}$	=	unsteady aerodynamic loads
N_f	=	degree of freedom of system
$\mathbf{\Psi}_r$	=	r-order proper orthogonal decomposition basis
H_g	=	nondimensional gust wavelength
L_{ref}	=	characteristic length

I. Introduction

In flight, aircraft commonly encounter atmospheric turbulence and gusts. Gusts are treated for linear analysis as a set of fluctuations in the flow velocity around the background steady state. During gusts encounter, the forces and moments acting on the aircraft change rapidly, in turn exciting rigid and flexible dynamic responses of the entire aircraft [1]. The dynamic response to gusts can lead to passengers' discomfort, overstress structural components above the design target loads, and, in some cases, cause structural failure [2].

Gust alleviation using active control is a promising and attractive technology because it can simultaneously reduce the weight and increase the performance of modern aircraft. One key issue for gust alleviation technology is to establish an efficient, high fidelity aero-servo-elastic (ASE) model used for active control design. Generally, ASE studies have used low fidelity linear aerodynamic models, including lifting surface theory, piston theory, quasi-steady aerodynamics, and the doublet-lattice method [3]. For an incompressible, irrotational and two-dimensional flow around a flat plate, Theodorsen [4] provides an analytical formulation of the unsteady aerodynamic loads. The Wagner function [5] describes the indicial built-up of the circulatory part of the lift, including the influence of the shed wake. The Küssner function [5] gives the lift built-up for the penetration into a sharp-edge gust. For a moving sharp-edge gust, in which the gust front moves towards or away from the aerofoil, an analytical formulation is given in Ref. [6]. Exact analytical expressions of the indicial response to a step change in angle of attack, a step change in pitch rate, and for the penetration into a sharp-edge gust in subsonic compressible flow were obtained by Lomax [7]. For a compressible flow, there are no exact closed-form analytical solutions for all times.

At transonic speed, the flow is dominated by nonlinear effects and exhibits complex interactions between shock waves and boundary layer. High fidelity models based on computational fluid dynamics (CFD) are instrumental to tackle critical flow conditions used for structural sizing of aircraft components, involving transonic as well as massively separated flows. For gust simulation, the field velocity method [8, 9] was introduced to extend the unsteady CFD analysis to gust simulation. This method was validated by the calculation of the indicial, stationary gust responses [9, 10], moving gust [8], and was also applied in a complex aircraft analysis [11].

High fidelity ASE models, based on coupling a CFD solver with a computational structural dynamics (CSD) solver, are used for accurate time marching. Two considerations are worth noting about the application of coupled CFD/CSD methods for active flutter suppression (AFS) problems: first, the computational cost of coupled simulations for three-dimensional (3D) configurations is today unrealistic for practical applications despite the availability of high performance computing (HPC) facilities; second, a low-dimensional state space model is needed for the control design synthesis. To find a compromise between these two contrasting requirements, model reduction techniques aim at balancing high fidelity and low cost/dimensionality. Several reduced order models (ROMs) methods have been developed for gust responses. System identification and manipulation of the governing equations are the two main methods to derive a ROM. System identification methods [12-16] take the response of the system to known inputs. These methods have been applied successfully, the disadvantages of these methods are the lack of a general robust parameterization of the model and the inability to predict any physics that is not included in the training data. The second approach is to manipulate the governing equations. For example, the harmonic balance [17] and the nonlinear model projection [1, 10, 18] have been applied to a variety of test cases and models. The latter method, in particular, is well suited to control synthesis design

for gust loads alleviation. A novel approach to the reduction of nonlinear models for gust loads prediction was first introduced in Ref. [10]. The method uses information on the eigenspectrum of the coupled system Jacobian matrix and projects the full order model through a series expansion onto a small basis of eigenvectors which is capable of representing the full order model dynamics. Linear and nonlinear ROMs derived from linear unsteady aerodynamics/CFD and linear/nonlinear structural models were generated. The application to the Goland wing was documented in Ref. [1], and that to a complete aircraft configuration in Ref. [18]. The method has several strengths, namely: (i) that it exploits information from the stability (flutter) calculation for the development of a ROM for dynamic response analyses; (ii) linear or nonlinear reduced models can be developed within the same framework; and (iii) the reduced model can be parametrised to avoid ROM regeneration.

Alternative methods based on proper orthogonal decomposition (POD) have also been used to generate CFD-based ROMs. References [19] and [20], respectively, performed AFS and control design for gust loads alleviation using a POD ROM, and a balanced truncation (BT) method was applied to further reduce the dimension of the time-domain POD ROM. The controller designed using the POD ROM showed good performance in AFS and gust alleviation, but in their method [20], the authors simplified the gusts into uniform field velocity and ignored the gusts penetration effects. Reference [21] presented the development of a CFD-based gust model for the Boeing truss braced wing aircraft. The ROM combines the convolution of a sharp-edge gust with a model constructed from the POD of the covariance matrix of the sharp-edge gust unsteady pressure coefficients. The ROM was found in good agreement with the CFD solution for a one-minus-cosine gust, and was then employed to compute at no extra cost a family of one-minus-cosine gust responses. Reference [22] investigated the POD ROM method to compute the aerodynamic and structural response to gust encounter. To consider the non-uniform velocity distribution of gust

simulation in ROM, the snapshots of POD method in their method were calculated in frequency domain based on linearised approach at non-uniformly distributed frequencies.

The main contribution of this paper is the development of a ROM derived from a coupled CFD/CSD system for gust loads analysis. The work is centred around two objectives. The first is the extension and application of an approach to introduce gust disturbances in a ROM, which has been previously investigated for a two-dimensional rigid aerofoil problem [23]. The second objective is to perform the control design synthesis on a ROM in state space form that enables the use of modern control theory without extra complications. The work is demonstrated on two test cases, including a typical wing section and the AGARD 445.6 wing.

The paper continues in Section II with a description of computational fluid dynamics solver and the gust ASE ROM construction method based on CFD. Then, Section III concerns with the open- and closed-loop gust responses. Finally, conclusions are given in Section IV.

II. Formulation

A. Full Order Model

The CFD solver is based on a finite volume, multi-block structured solver. The unsteady Reynolds-averaged Navier-Stokes equations (URANS) are solved using a cell-centered approach. The spatial discretization is based on the second order Van Leer scheme [24]. For time marching, the lower-upper symmetric Gauss-Seidel (LU-SGS) method is employed. For aeroelastic calculations, the interpolation using surface splines (IPS) method [25] allows transferring applied forces from the aerodynamic domain to the structural domain. The aerodynamic mesh deformation is obtained through radial basis functions combined with the transfinite interpolation method [26, 27]. In this work, the test cases are for a wing typical section, with the structural model represented by two springs in pitch (torsional mode) and plunge (bending mode) with linear stiffness, and for

the AGARD 445.6 wing, where the modal model consists of four structural modeshapes. The interested reader is referred to Ref. [28] for more details on the underlying methodology, the CFD/CSD coupling, and validation cases for steady and unsteady problems.

For gust analysis using CFD, the field velocity approach [9] is used. The gust is introduced into the CFD analysis by modification of the velocity of grid points during the unsteady motion of the aircraft. Further use and development of this method have been performed in Refs. [23] and [29]. An advantage of the field velocity approach is that it overcomes the problems associated with the numerical dissipation of the disturbance, and no requirements on the spatial discretisation exist. A disadvantage is that the gust is assumed frozen, and the influence of the structural response on the gust is neglected. This assumption loses validity when second order effects, which occur in extreme flight conditions at the edges of the envelope, become important. The approach, however, has received widespread use because of the lack of alternative methods.

B. Reduced Order Model

The generation of the ROM for gust analysis and load alleviation consists of three steps. The first is the derivation of a ROM from the unsteady flow solver. The second step is coupling the unsteady aerodynamic ROM with an adequate structural dynamics model to obtain a complete ASE ROM. Finally, the coefficients representing the impact of discrete gust and continuous turbulence on the ROM response are calculated. A short description of each step follows.

1. Unsteady Aerodynamic Reduced Order Model

The discrete system of nonlinear equations [30] in the time domain using an Arbitrary Lagrangian-Eulerian formulation is:

$$\frac{d(\mathbf{A}(\mathbf{u},\alpha,\delta)\,\mathbf{w})}{dt}+\mathbf{F}(\mathbf{w},\mathbf{u},\alpha,\delta)=\mathbf{0} \tag{1}$$

where $\mathbf{w}(t)$ denotes the vector of conservative flow variables, $\mathbf{u}(t)$ represents the structural motion, and $\delta(t)$ indicates the control surface deflection. The nondimensional time is denoted by *t*. The volume of the fluid cell is denoted by **A**, and **F** indicates, in the current work, the inviscid flux resulting from the spatial discretization. Herein, the parameter $\alpha(t)$ is a measure of the angle of attack, which is used to introduce the gust terms in the ROM [23]. The nonlinear fluid equations are linearised about an operating point where a base nonlinear solution is computed first [28, 30]:

$$\begin{aligned}\dot{\mathbf{w}} &= \mathbf{A}\mathbf{w}+\mathbf{B}\mathbf{x}_s(t)+\mathbf{D}g(t)+\mathbf{E}\delta(t)\\ \mathbf{y} &= \mathbf{C}\mathbf{w}\end{aligned} \tag{2}$$

where $\mathbf{x}_s(t)=[\mathbf{u},\dot{\mathbf{u}}]^{\mathrm{T}}$, $\mathbf{A}=-\mathbf{A}_0^{-1}\dfrac{\partial\mathbf{F}}{\partial\mathbf{w}}$, $\mathbf{B}=-\mathbf{A}_0^{-1}\left[\dfrac{\partial\mathbf{F}}{\partial\mathbf{u}}\quad \mathbf{w}_0\dfrac{\partial\mathbf{A}}{\partial\mathbf{u}}+\dfrac{\partial\mathbf{F}}{\partial\dot{\mathbf{u}}}\right]$, $\mathbf{C}=\dfrac{\partial\mathbf{f}^{ext}}{\partial\mathbf{w}}$,

$$\mathbf{D}=-\mathbf{A}_0^{-1}\left[\frac{\partial\mathbf{F}}{\partial\alpha}\quad \mathbf{w}_0\frac{\partial\mathbf{A}}{\partial\alpha}+\frac{\partial\mathbf{F}}{\partial\dot{\alpha}}\right],\ \mathbf{E}=-\mathbf{A}_0^{-1}\frac{\partial\mathbf{F}}{\partial\delta},\ g(\mathrm{t})=[\alpha(t),\dot{\alpha}(t)]^{\mathrm{T}},\ \mathbf{y}=\mathbf{f}^{\mathrm{ext}}(t)-\mathbf{f}_0^{\mathrm{ext}}(t_0)$$

$\mathbf{A}_0$ is the fluid cell volume for the (initial) undeformed configuration, and $\mathbf{f}_0^{\mathrm{ext}}$ is the vector of aerodynamic forces at the steady state condition. The second set of equation, in Eq.(2), relates the flow solution to the aerodynamic quantities of interest, i.e. distributed surface quantities (pressure coefficient, etc.) and/or integrated ones (generalised forces and moments, etc.). Equation (2) represents the full order linearised time domain (LTD) aerodynamic model in state-space form. The LTD model retains the same size of the full order model that may consist, generally, of several million degrees of freedom. The main drawback is that the LTD is too large for fast predictions of the unsteady aerodynamic forces and not ideal for gust load alleviation and multidisciplinary design. To achieve a significant reduction on the size of the model, the POD technique [28] is employed. The POD technique is a system optimization method to extract a small basis of modes,

$\boldsymbol{\Psi}_r$, that represent the dynamics of the original model. Then, the vector of degrees of freedom of the full order model, **w**, is projected onto the basis of POD modes:

$$\mathbf{w} = \boldsymbol{\Psi}_r \mathbf{w}_r \tag{3}$$

The number of modes used in an aeroelastic problem was studied in Ref. [28]. By projecting the LTD model onto the subspace $\boldsymbol{\Psi}_r$, the set of equations in Eq. (2) rewrites as:

$$\begin{aligned} \dot{\mathbf{w}}_r &= \mathbf{A}_a \mathbf{w}_r + \mathbf{B}_a \mathbf{x}_s(t) + \mathbf{D}_a g(t) + \mathbf{E}_a \delta(t) \\ \mathbf{y} &= \mathbf{C}_a \mathbf{w}_r \end{aligned} \tag{4}$$

where $\mathbf{A}_a = \boldsymbol{\Psi}_r^{\mathrm{T}} \mathbf{A} \boldsymbol{\Psi}_r$, $\mathbf{B}_a = \boldsymbol{\Psi}_r^{\mathrm{T}} \mathbf{B}$, $\mathbf{C}_a = \mathbf{C} \boldsymbol{\Psi}_r$, $\mathbf{D}_a = \boldsymbol{\Psi}_r^{\mathrm{T}} \mathbf{D}$, $\mathbf{E}_a = \boldsymbol{\Psi}_r^{\mathrm{T}} \mathbf{E}$.

The size of the unsteady aerodynamic ROM in Eq.(4) is *r*, typically in the order of 10^1-10^2, which is much smaller than the size of LTD described in Eq.(2), often larger than 10^6. The vectors $g(t)$ and $\delta(t)$ are the system inputs, and $\mathbf{w}_r \in \mathbf{R}^{r\times 1}$ is the state space vector of the ROM.

2. Aeroservoelastic Reduced Order Model

The structural dynamic equations in modal coordinates are formulated as [28]:

$$\begin{aligned} \dot{\mathbf{x}}_s(\tau) &= \mathbf{A}_s \mathbf{x}_s(\tau) + q\mathbf{B}_s \left(\mathbf{f}^{ext}(\tau) - \mathbf{f}_0^{ext}(\tau) \right) \\ \mathbf{u} &= \mathbf{C}_s \mathbf{x}_s(\tau) \end{aligned} \tag{5}$$

where $\mathbf{A}_s = \begin{bmatrix} \mathbf{0} & \mathbf{I} \\ -\bar{\mathbf{M}}^{-1}\bar{\mathbf{K}} & -\bar{\mathbf{M}}^{-1}\bar{\mathbf{G}} \end{bmatrix}$, $\mathbf{B}_s = \begin{bmatrix} \mathbf{0} \\ \bar{\mathbf{M}}^{-1} \end{bmatrix}$, $\mathbf{x}_s = \left[\mathbf{u}, \dot{\mathbf{u}}\right]^{\mathrm{T}}$, $\mathbf{C}_s = \mathbf{I}$. The matrices $\bar{\mathbf{M}}$, $\bar{\mathbf{G}}$ and $\bar{\mathbf{K}}$ are, respectively, the generalised mass, damping and stiffness matrices.

Comparing Eq.(4) and Eq.(5), one finds that the aerodynamic and structural models are formulated using a different definition of the time scale. In particular, the nondimensional time of the aerodynamic model, *t*, is related to the dimensional time of the structural model, τ, by the

relation $t = \tau \mathrm{V}/L_{ref} = \tau/\omega$. Rewrite Eq.(4) in terms of *t*, and then substitute the variable $\mathbf{w}_r$ with $\mathbf{x}_a$ for consistency with Eq.(5). It follows that the unsteady aerodynamic ROM is:

$$\begin{aligned}\dot{\mathbf{x}}_a(\tau) &= \mathbf{A}_a\mathbf{x}_a(\tau)/\omega + \mathbf{B}_a[\mathbf{u}(\tau)/\omega, \dot{\mathbf{u}}(\tau)]^{\mathrm{T}} \\ &\quad + \mathbf{D}_a[\alpha(\tau)/\omega, \dot{\alpha}(\tau)]^{\mathrm{T}} + \mathbf{E}_a\,\delta(\tau)/\omega \\ \mathbf{y}(\tau) &= \mathbf{C}_a\mathbf{x}_a(\tau)\end{aligned} \tag{6}$$

The resulting ASE ROM in state space form is obtained coupling Eqs.(5) and (6):

$$\begin{aligned}\dot{\mathbf{x}}_{ase}(\tau) &= \mathbf{A}_{ase}\mathbf{x}_{ase}(\tau) + \mathbf{B}_{ase}g(\tau) + \mathbf{D}_{ase}\delta(\tau) \\ \mathbf{y}_{ase}(\tau) &= \mathbf{C}_{ase}\mathbf{x}_{ase}(\tau)\end{aligned} \tag{7}$$

where $\mathbf{x}_{ase} = [\mathbf{x}_a, \mathbf{x}_s]^{\mathrm{T}}$, $y_{ase} = \mathbf{x}_s$, $\mathbf{A}_{ase} = \begin{bmatrix} \mathbf{A}_a/\omega & \mathbf{B}_a(:,1:n)/\omega & \mathbf{B}_a(:,n+1:2n) \\ q\cdot\mathbf{B}_s\mathbf{C}_a & & \mathbf{A}_s \end{bmatrix}$,

$\mathbf{B}_{ase} = \begin{bmatrix} \mathbf{D}_a(:,1)/\omega & \mathbf{D}_a(:,2) \\ \mathbf{0} & \end{bmatrix}$, $\mathbf{D}_{ase} = \begin{bmatrix} \mathbf{E}_a/\omega \\ \mathbf{0} \end{bmatrix}$, $\mathbf{C}_{ase} = [\mathbf{0}, \mathbf{C}_s]$, $g(\tau) = [\alpha(\tau)/\omega, \dot{\alpha}(\tau)]^{\mathrm{T}}$

$y_{ase}(\tau)$ is the vector of the structural motions and velocities in modal coordinates. The size of the ASE system in Eq.(7) is $N_{dof} = r + 2n$, which consists of *r* POD modes and *n* structural modeshapes. The factor of 2 accounts for rewriting the structural problem in state space form.

3. Gust Treatment In Reduced Order Model

A different method from the grid velocity approach is used to introduce gust effects in the ROM framework. We start observing that any disturbance, representing both discrete gusts and continuous turbulence, appears in the ROM equations through the term $g(\tau) = [\alpha(\tau)/\omega, \dot{\alpha}(\tau)]^{\mathrm{T}}$. In Ref. [23], we have presented a new methodology that builds on two requirements: speed and simplicity. The first consideration is to avoid degrading the computational performance of the ROM for gust analysis. The second consideration of simplicity is inspired by the Küssner function that gives the lift built up for a sharp-edged gust. The detailed derivation process can be referenced

in [21]. Whereas Ref. [23] presented a thorough validation and verification exercise for a rigid aerofoil, the methodology is herein extended to 2D and 3D aeroelastic test cases.

We proposed to model the angle of attack due to a moving sharp-edge gust of intensity $\hat{w}_{g0} = w_{g0}/U_\infty$ as:

$$\alpha_{SE}(\tau) = \hat{w}_{g0} c(1 - \mathrm{e}^{-\beta\tau}), \qquad 0 < \tau < \frac{\mathrm{L}_g}{U_\infty \lambda^{-1}} \tag{8}$$

where c and β are parameters to be identified once during the ROM generation. The term λ is the advance ratio [6], defined as:

$$\lambda = \frac{V}{V + u_g} = \frac{M}{M + u_g/a} \tag{9}$$

where u_g is the horizontal component of the gust velocity. The parameter c is identified from the relation:

$$c = \frac{C_L(\tau_f)}{C_L^{\mathrm{ROM}}(\tau_f, \beta = 0, c = 1)} \tag{10}$$

where the steady state response, at the final time $\tau_f = N\Delta\tau$, to a sharp-edged gust computed using the original CFD solver, C_L, is compared with that computed using the ROM, C_L^{ROM}. The parameter β rules the transient response and is calculated from a minimization problem carried out in time:

$$f = \min_{\beta} \sum_{i=0}^{N} \left(C_{Li} - C_{Li}^{\mathrm{ROM}}(\beta) \right)^2 \tag{11}$$

Equation (8) is used in this work to evaluate the effects of the encounter with a sharp-edge gust within a ROM analysis. To calculate the response to any arbitrary gust shape, indicial

aerodynamics is then used. Applying the convolution integral for an arbitrary-shaped gust, $\hat{w}_g$, one obtains the gust term which provides the forcing function of the ASE ROM in Eq. (7):

$$\alpha(\tau) = \int_0^\tau \frac{d\hat{w}_g(t)}{dt} \alpha_{SE}(\tau - t)\,\mathrm{d}t \tag{12}$$

C. Control Design on ROM

A linear quadratic regulator (LQR) is designed for the single-input, multi-output system represented by the ROM of Eq. (7). The LQR control problem, assuming the entire state vector accessible for feedback, seeks a linear control law of the form:

$$\delta(\tau) = -\mathbf{K}^* \mathbf{x}_{ase}(\tau) \tag{13}$$

where **K*** is a suitable control matrix. In practice, a suboptimal control problem is formulated as a practical alternative when only few elements or few linear combinations of the elements in the state vector are accessible for feedback control. This aspect is further discussed in the definition of each test case. Setting $\mathbf{K} = \mathbf{K}^* \mathbf{C}_{ase}^{\mathrm{T}} / \left(\mathbf{C}_{ase} \mathbf{C}_{ase}^{\mathrm{T}} \right)$, the output vector feedback control law is formulated as:

$$\delta(\tau) = -\mathbf{K}\mathbf{C}_{ase}\mathbf{x}_{ase}(\tau) = -\mathbf{K}\mathbf{y}_{ase}(\tau) \tag{14}$$

The LQR control problem seeks a gain matrix **K** to minimise a specified performance criterion expressed here as:

$$J = \sum_{k=0}^{\infty} \left\{ \mathbf{x}_{ase}^{\mathrm{T}}[k] \mathbf{Q} \mathbf{x}_{ase}[k] + \delta^{\mathrm{T}} \mathbf{R} \delta[k] \right\} \tag{15}$$

where **Q**, referred to as the state weighting matrix, is a symmetric semi-positive definite matrix, and **R**, referred to as the control weighting matrix, is symmetric and positive definite. The optimum gain matrix is obtained solving numerically the set of equations:

$$\mathbf{K} = \mathbf{R}^{-1}\mathbf{B}\mathbf{P}$$
$$\mathbf{P}\mathbf{A} + \mathbf{A}^{\mathrm{T}}\mathbf{P} - \mathbf{P}\mathbf{B}\mathbf{R}^{-1}\mathbf{B}^{\mathrm{T}}\mathbf{P} + \mathbf{Q} = \mathbf{0} \quad (16)$$

where **P** is the solution of the Riccati equations. In this work, the Riccati equations and the optimal gain matrix are calculated using the built-in functions of Matlab/SIMULINK (version R2016a).

III. Results

A. Wing Typical Section

The first test case is for a wing typical section with a trailing edge control surface located at three-quarter of the chord from the leading edge. The pitch and plunge degrees of freedom are restrained by a set of elastic springs with linear stiffness. The aerofoil section is that of the NACA 0012 aerofoil. The aeroelastic parameters are summarised in Table 1.

Table 1. Aeroelastic parameters of the NACA0012 aerofoil

Parameter	ω_h/ω_α	μ	a	x_α	r_α^2
Value	0.342	100	-0.2	0.2	0.539

The grid used in this work consists of 11020 cells with 230 nodes distributed on the aerofoil surface. The grid was chosen after a convergence study solving the Euler equations, and the interested reader may find more details on the background studies in a previous work [28].

1. Aeroservoelastic Reduced Order Model

The generation of the ROM is detailed, and some examples are given for validation. First, the LTD model is obtained around a steady state condition, α = 0 deg. Then, a number of POD modes is extracted from an unsteady time domain analysis using the LTD model. The training data were

obtained by applying an impulse individually to structural modal coordinates and corresponding velocities. The choice of the impulse function reflects the ability to excite relevant unsteady aeroelastic characteristics. The basis of POD modes used for the projection of the LTD model was chosen to guarantee that 99.99% of the total energy of the system was retained after the truncation [28]. Finally, the calculation of the gust terms in the ROM, c and β in Eq. (8), requires simulating the CFD response to a stationary sharp-edge gust (with $\hat{w}_{g0} = 0.0349$). Table 2 summarises the gust terms computed at various Mach numbers. The resulting ASE ROM contains 54 states, including 50 POD modes as detailed in Ref. [23] and 4 states for the state-space representation of the pitch and plunge dynamics. On the contrary, the full order model, from which the ASE ROM is derived, consists of 55114 DoFs (55110 fluid and 4 structural DoFs).

Table 2. Gust terms for the ROM of the wing typical section ($\alpha = 0$ deg, $\hat{w}_{g0} = 0.0349$)

M	c	β
0.3	0.9574	0.44
0.5	0.9613	0.75
0.7	0.9979	1.02
0.8	1.0335	0.92

The ability to predict correctly the gust encounter is instrumental for an accurate analysis of the gust effects before any active control strategy can be developed. A number of test cases were run to validate the unsteady aerodynamic ROM for a set of moving sharp-edge gusts. The indicial responses computed from the CFD solver (55100 DoFs) and the unsteady aerodynamic ROM (50 DoFs) for the rigid aerofoil are compared in Figure 1. The agreement is good for all test cases. It is worth observing that the case $\lambda = 0$ represents the response to a step change in angle of attack,

and that $\lambda = 1$ represents the response to a sharp-edge gust with a front moving downstream at the freestream speed.

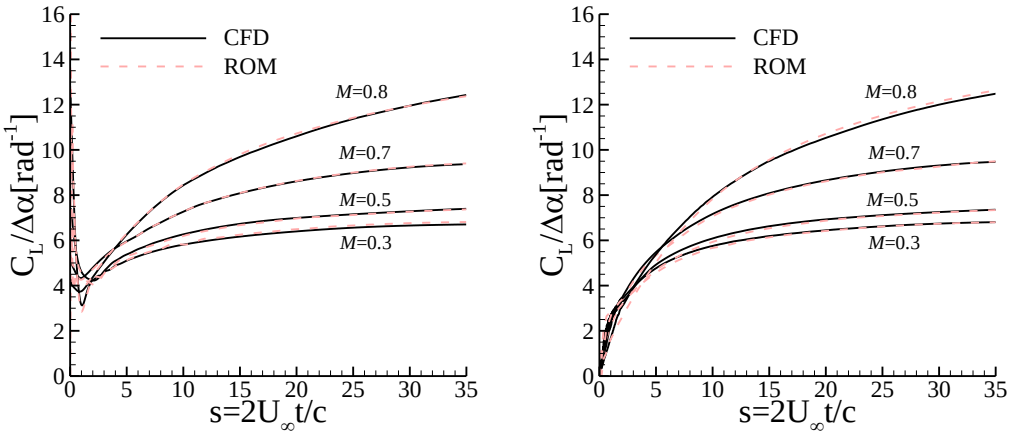

(a) $\lambda = 0$ (step change in angle of attack) (b) $\lambda = 1$ (sharp-edge gust)

Figure 1. Indicial response of lift coefficient to a moving sharp-edge gust for the wing typical section

(α = 0 deg, $\hat{w}_{g0} = 0.0349$)

2. Open-loop Response

At *M* = 0.7, the flutter speed is found at a reduced velocity VF = 3.7935. The tracing of the eigenvalue of the aeroelastic system with the largest real part is shown in Figure 2. The flutter calculation was performed using the full order CFD/CSD model. For the results of the wing typical section herein discussed, a flight condition was chosen at V = 2.0 for *M* = 0.7, which is within the flutter boundary and the aeroelastic system is asymptotically stable.

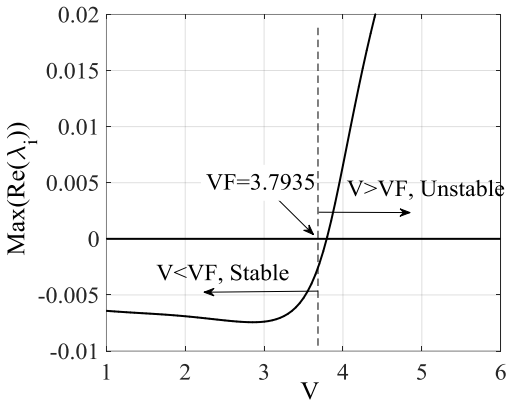

Figure 2. Dependence of the aeroelastic eigenvalue with the largest real part on reduced speed

($M = 0.7$, $\alpha = 0$ deg)

Having tested the ROM, the worst case gust search was performed for the one-minus-cosine gust, defined here as:

$$\hat{w}_g(x_g) = \frac{\hat{w}_{g0}}{2}\left(1 - \cos\frac{2\pi x_g}{H_g}\right), \qquad 0 \le x_g \le H_g \tag{17}$$

where x_g is the position of the aircraft in the spatial description of the gust relative to a convenient fixed origin, and H_g is the gust wavelength normalised by the aerofoil semi-chord.

The search domain was divided into 100 design sites with $H_g \in [1,100]$. As a model problem, the worst case gust was defined as the gust causing the largest response in the pitch DoF. Figure 3 reports the profiles identifying the largest deformations in pitch and plunge. The worst case gust for the pitch degree of freedom was found for a nondimensional wavelength $H_g = 10$ as this matches the frequency of the pitch mode. The time response corresponding to the worst case gust is shown in Figure 4, which conveys the good predictive capability of the ASE ROM compared with the full order simulation. The computing time to carry out the worst case gust search was

about 16 seconds using the ASE ROM, while the same search based on the full order CFD/CSD would have taken over 70 h (40 min per CFD/CSD simulation, for 100 design points).

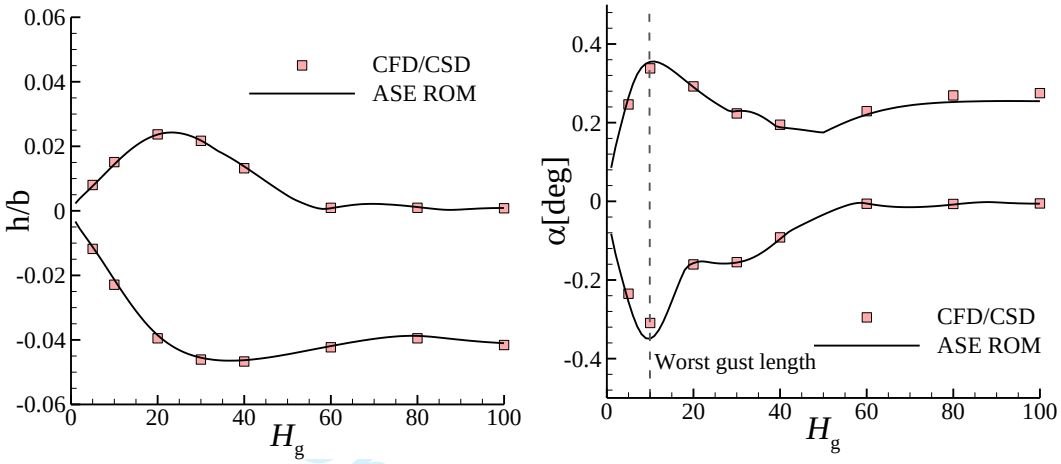

(a) Nondimensional plunge (b) Pitch

Figure 3. Worst case gust search of H_g for the wing typical section to one-minus-cosine gust family ($M = 0.7$, V = 2.0, $\hat{w}_{g0} = 0.0349$, $\lambda = 1$)

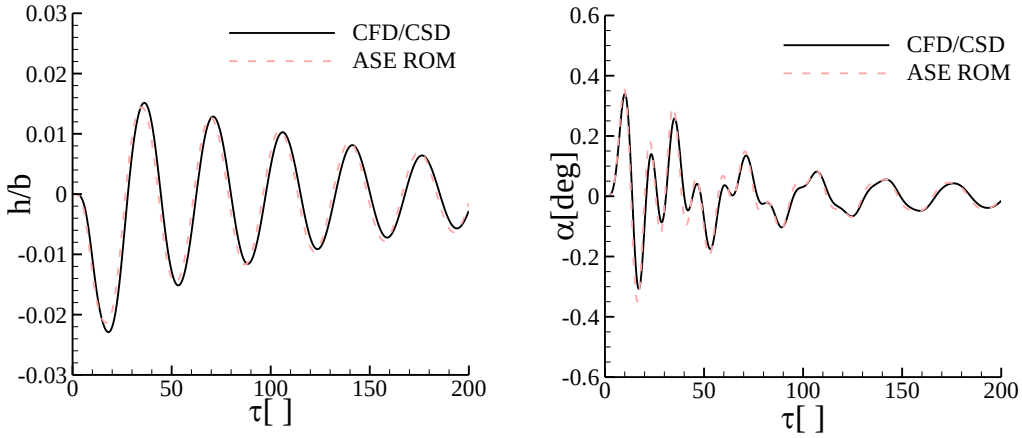

(a) Nondimensional plunge (b) Pitch

Figure 4. Time domain (open-loop) response for the wing typical section corresponding to the worst case one-minus-cosine gust ($M = 0.7$, V = 2.0, $\hat{w}_{g0} = 0.0349$, $\lambda = 1$)

Once the ROM is generated, it can be used to analyse the aeroelastic response to any synthetic gust shape at no extra costs. As an example, Figure 5 illustrates the worst case gust profiles (for a gust wavelength $H_g = 10$) considering the advance ratio, λ, as the independent parameter. Several calculations from the full order CFD/CSD model confirm the predictive capability of the ROM. It was already observed and proved in a previous work [23] that a change in the advance ratio, for a given H_g, corresponds to a change in the effective gust wavelength. Therefore, it is not unexpected that for the previously identified worst case gust ($H_g = 10$), the critical advance ratio is $\lambda = 1$. For reference, however, Figure 6 reports the aeroelastic responses computed at various advance ratios. The agreement of the ASE ROM with the full order results is good for all times, including the gust-aerofoil interaction for smaller times, and when the gust moves away from the aerofoil for larger times.

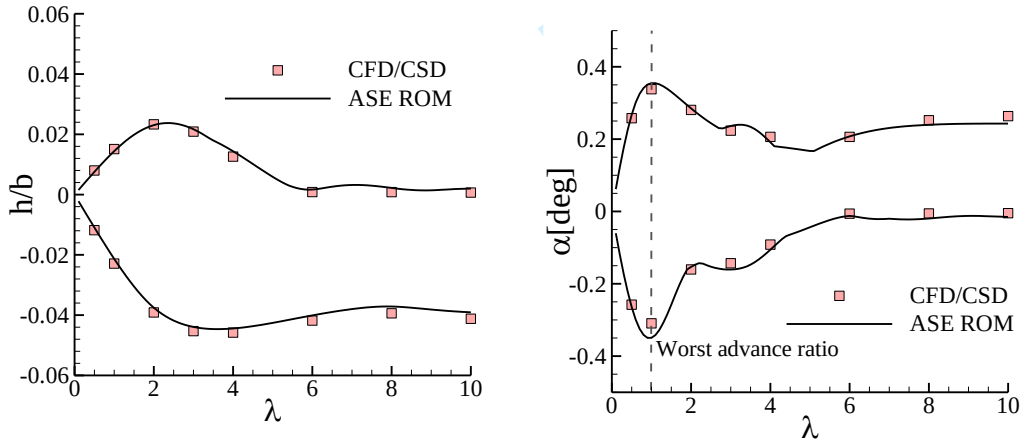

(a) Nondimensional plunge (b) Pitch

Figure 5. Worst case gust search of λ for the wing typical section to one-minus-cosine gust family

($M = 0.7$, V = 2.0, $H_g = 10$, $\hat{w}_{g0} = 0.0349$)

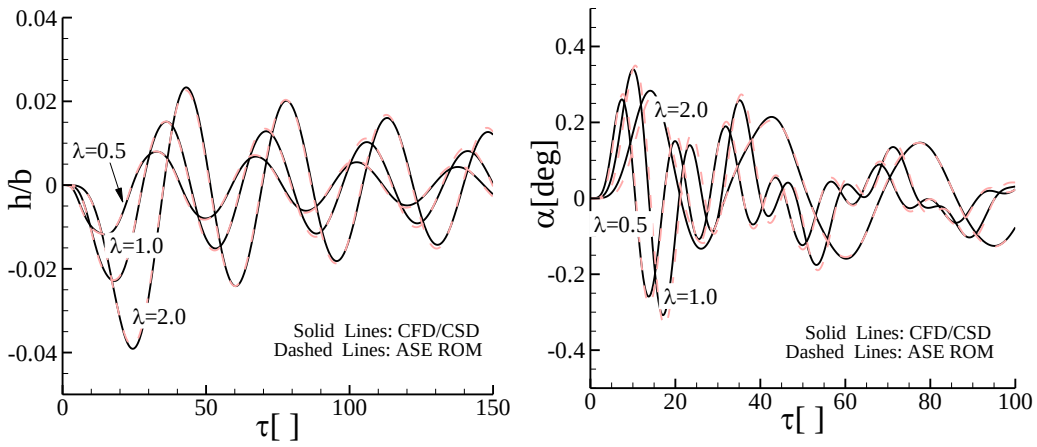

(a) Nondimensional plunge (b) Pitch

Figure 6. Time domain (open-loop) responses for the wing typical section to one-minus-cosine gust at various advance ratios ($M = 0.7$, V = 2.0, $H_g = 10$, $\hat{w}_{g0} = 0.0349$)

The aeroelastic response to continuous turbulence is also of relevance as prescribed by certification authorities. Here, a time domain signal for the Dryden model [31, 32] was generated, but the same could have been done with the Von Karman spectrum. Calculations were run for a total nondimensional time of 1000, and the turbulence was introduced for the first 400 nondimensional time units. The aeroelastic responses as calculated by the full order model and the ASE ROM are shown in Figure 7. It was found that the structural motion remains small during the entire simulation, with small changes also affecting the instantaneous flow field around the mean flow. The comparison between the two models is satisfactory.

An advantage of the ROM is the high computational efficiency compared to the CFD model. For example, results in Figure 7 were computed for 1000 nondimensional times. The unsteady analysis using the full order model requires about 3202 seconds. For the same settings, once the ROM is generated, the time integration of the ASE ROM requires about 5 seconds, with a speedup higher than two orders of magnitude.

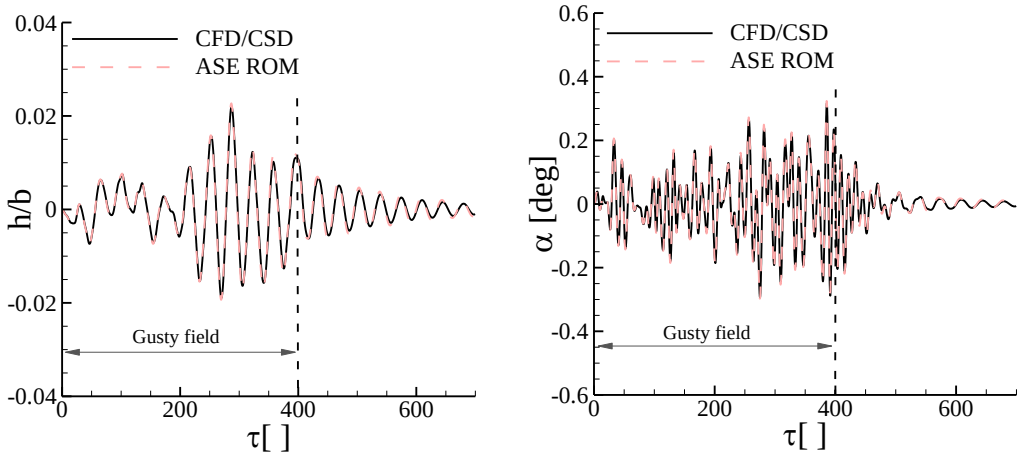

(a) Nondimensional plunge (b) Pitch

Figure 7. Time domain (open-loop) responses for the wing typical section to continuous turbulence (Dryden, M = 0.7, V = 2.0)

3. *Closed-loop Response*

This section concerns the validation of the LQR-based control law that was designed using the ASE ROM as the system to be controlled. The control design was exercised at the flight condition V = 2.0 for M = 0.7. It was assumed that the pitch and plunge, and their respective velocities, were accessible. The state and control weighting matrices were set to $\mathbf{R}$ = 1 and $\mathbf{Q}$ = $\mathbf{I}$, where $\mathbf{I} \in R^{54} \times R^{54}$. Once the controller was designed, it was first tested on the ASE ROM and then applied on the full order model. The comparison conveys indications of the impact on control effectiveness when the LQR is transferred from the ROM to the full order model. In all cases, a good to excellent comparison was found, and for convenience the responses of the full order model are analysed in the following paragraphs.

The first validation test case is for the worst case gust of one-minus-cosine shape, with parameters $H_g = 10$, $\hat{w}_{g0} = 0.0349$ and $\lambda = 1$. The open- and closed-loop responses of the full order model are reported in

Figure 8. From the comparison, it is found that the controller, which was designed using the ASE ROM, is effective in alleviating the aeroelastic response when applied to the original coupled CFD/CSD model.

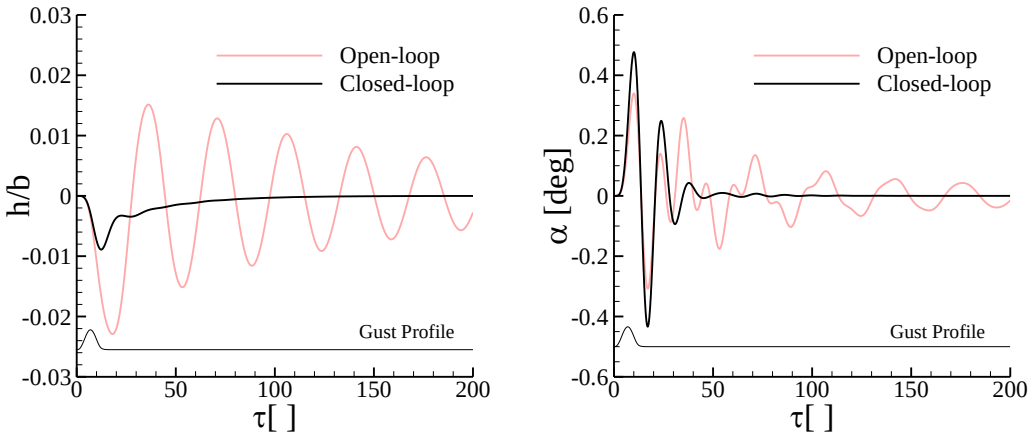

(a) Nondimensional plunge (b) Pitch

Figure 8. Open- and closed-loop responses computed by the coupled CFD/CSD method for the wing typical section to one-minus-cosine gust ($M = 0.7$, V = 2.0, $H_g = 10$, $\hat{w}_{g0} = 0.0349$, $\lambda = 1$)

The second test case concerns the use of the same control algorithm to suppress the aeroelastic response following the encounter with a continuous turbulence (Dryden model). Results are shown in Figure 9. Comparing the open- and the closed-loop responses evinces the ability of the controller to reduce the gust response. In particular, the standard deviation of the vibrations in the plunge DoF was reduced from 0.00747 to 0.00172, corresponding to a 77% reduction. The effect of the active control is minimal on the pitch DoF, as this is the primary mechanism for loads alleviation via the trailing edge flap. Figure 10 reports the control input needed, comparing the results from the ASE ROM and the coupled CFD/CSD model. The two control input signals are nearly identical, confirming that the ASE ROM is adequate to synthetise a control algorithm which is then applied, for verification purposes, on the full model. Throughout the turbulence encounter, the largest

control deflection stays within ±2 deg, with a dominant reduced frequency content around 0.1. These values are realistic from a practical standpoint.

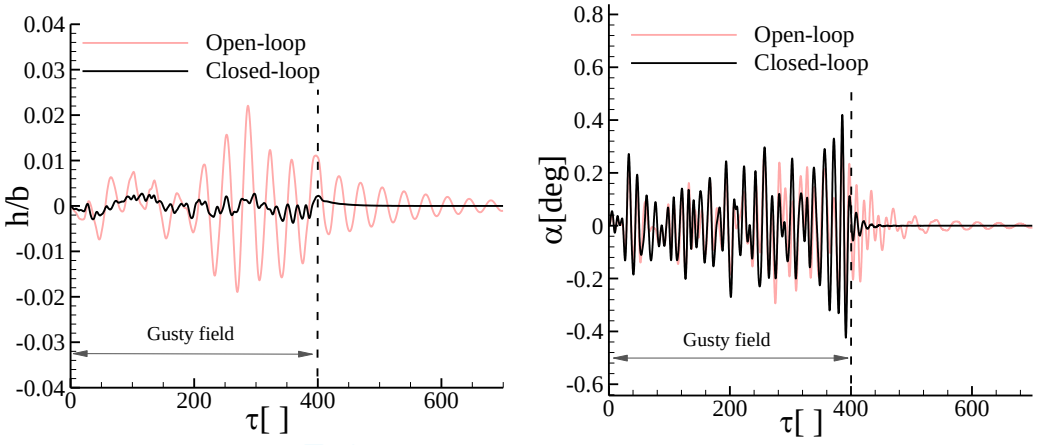

(a) Nondimensional plunge (b) Pitch

Figure 9. Open- and closed-loop responses computed by the coupled CFD/CSD method for the wing typical section to continuous turbulence (Dryden, $M = 0.7$, V = 2.0)

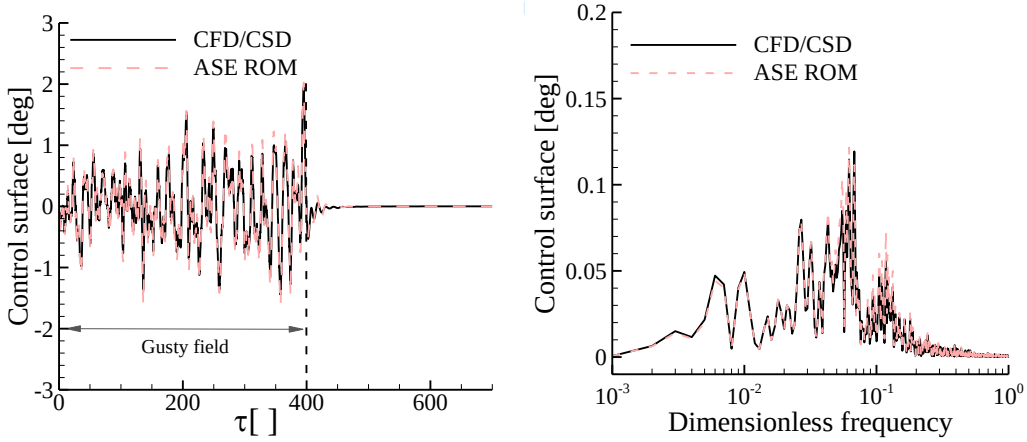

(a) Time domain response (b) Frequency content

Figure 10. Control action needed in the closed-loop response for the wing typical section to continuous turbulence (Dryden, $M = 0.7$, V = 2.0)

B. Three dimensional wing

The 3D test case is for the AGARD 445.6 wing [33] modified with a trailing edge control surface. The control surface is located on the outboard section of the wing from the wing tip, with dimensions equal to 20% of the wing span and 30% of the wing chord. The structural model uses the first four elastic modes, with frequencies f_1 = 9.46 Hz, f_2 = 39.71 Hz, f_3 = 49.51 Hz, and f_4 = 95.13 Hz. The motion of the control surface is modelled as an additional modeshape. The location and size of the control surface, the grid convergence study, the generation of the ROM and its use for flutter suppression were studied in Ref. [28], and follows closely what seen for the aerofoil test case above.

For this case, the freestream speed is set to V = 250 *m*/*s*, which is below the flutter speed of 288.4 *m*/*s* at M = 0.901 and $\rho = 0.0995 kg/m^3$. A feedback controller is designed using the ASE ROM derived from the POD BT. For the LQR synthesis, the model coordinates and their velocities are assumed accessible, and the weight matrices are set to R = 10 and $\mathbf{Q} = 0.1\,\mathbf{I}$, where $\mathbf{I} \in R^{58} \times R^{58}$.

The controller, which was designed using the ASE ROM of 60 DoFs, was then applied to the coupled CFD/CSD system, consisting of 1,012,850 DoFs. The response to a continuous turbulence modelled by Dryden spectrum is used as test case. The lift coefficient and the first modal coordinate of the open- and closed-loop responses are shown in Figure 11. For conciseness, only the coupled CFD/CSD responses are presented. It was found that the standard deviation of the first modal coordinate was reduced from 0.0081 to 0.0018, corresponding to a percentual reduction of about 78% when the feedback controller is on. The impact of reduced aeroelastic vibrations is evident on a similar reduction in the lift coefficient. The required control surface rotation is analysed in Figure 12. The rotation stays within ± 4 deg, with the largest frequency content around 15 Hz. These operating conditions are reasonable when confronted with the challenging flow conditions used in this test case (M = 0.901, V = 250 *m*/*s*).

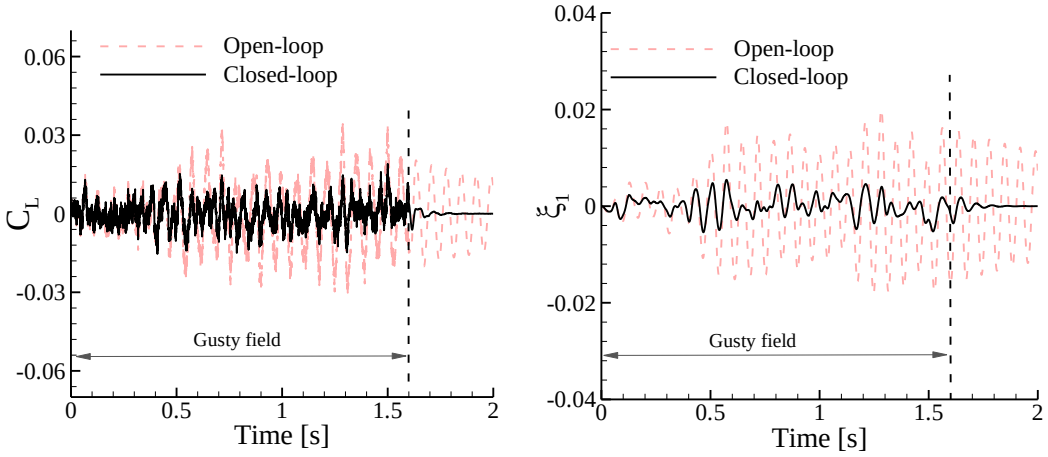

(a) Lift coefficient (b) First modal coordinate

Figure 11. Open- and closed-loop responses computed by the coupled CFD/CSD method for the modified AGARD 445.6 wing to continuous turbulence (Dryden, $M = 0.901$, V = 250 m/s)

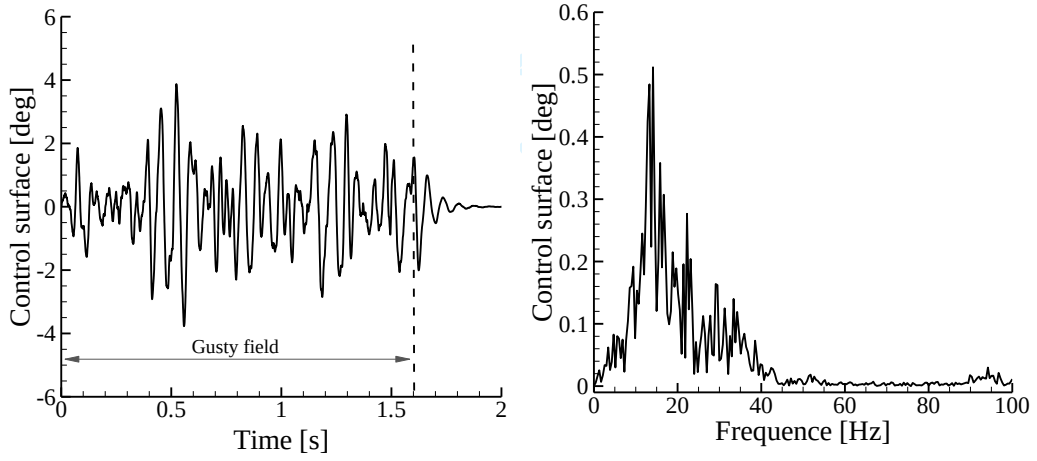

(a) Time history response (b) Frequency content

Figure 12. Control action needed in the closed-loop response computed by the coupled CFD/CSD method for the modified AGARD 445.6 wing to continuous turbulence (Dryden, $M = 0.901$, V = 250 m/s)

IV. Conclusions

This work reported on the development and application of a methodology for gust load alleviation using computational fluid dynamics as source of the aerodynamic predictions. The

methodology builds on two components. The first concerns the derivation of an aero-servo-elastic reduced order model. The model is obtained from the linearised flow solver, and a reduction in the model size is achieved through a proper orthogonal decomposition, further enhanced via a balanced truncation. Gust effects are modelled using an analytical formulation, with constants to be determined once during the model generation. The aerodynamic model thus obtained is then coupled with the structural dynamic model. The advantages of the aero-servo-elastic reduced order model are that: i) it is built around a nonlinear flow solution, accounting for the influence of shocks on the mean flow field; ii) once generated, the model allows investigating any gust shape, at no extra costs; and iii) it is formulated in a state-space form, which is suitable for both modern control theories and for a frequency domain analysis, if needed. The second component consists of performing control design synthesis directly on the model. This is straightforward, leveraging on the availability of a state-space model of small dimension, but raising the question about the validation of the control system. To this goal, once the controller is designed and tested on the reduced order model, it is implemented on the large computational coupled model for verification purposes.

Two configurations were considered in this work: a wing typical section and a modified AGARD 445.6 wing, both with a trailing edge control surface. Preliminary tests were run to ensure high quality of the reduced order model predictions consistently across different test cases. For the controller, a linear quadratic regular was used, assuming only that information on the structural motion was accessible for feedback. A number of gust shapes were analysed, including discrete and continuous functions. Comparisons between open- and closed-loop responses have revealed a significant gust load alleviation capability for both test cases. In particular, for a given continuous turbulence, the standard deviation of the loads and the structural motion were reduced by as much

as 77%. This is a good achievement as continuous turbulence, with a broad frequency content, is more challenging than discrete gusts and may impact negatively on the control effort needed.

Acknowledgments

This work was supported by the National Program on Key Research Project (No: MJ-2015-F-010), the National Natural Science Foundation of China (Nos. 11272005, 11472206, 11672225 and 11511130053), the Natural Science Foundation of Shaanxi Provence (No.2016JM1007),and the Basic Research foundations for the Central Universities (No.2014XJJ0126). Andrea Da Ronch acknowledges the financial support by the Royal Academy of Engineering under the Newton Research Collaboration Programme (NRCP1516/1/105).

References

[1] Da Ronch, A., N. Tantaroudas, S. Timme, and K. Badcock. *Model reduction for linear and nonlinear gust loads analysis*. in *54th AIAA/ASME/ASCE/AHS/ASC Structures, Structural Dynamics, and Materials Conference*. 2013. Boston, MA. DOI: 10.2514/6.2013-1492

[2] Noll, T.E., J.M. Brown, M.E. Perez-Davis, S.D. Ishmael, G.C. Tiffany, M. Gaier, and N. Headquarters, *Investigation of the Helios Prototype Aircraft Mishap, Volume I Mishap Report.* 2012.

[3] Regan, C.D. and C.V. Jutte, *Survey of Applications of Active Control Technology for Gust Alleviation and New Challenges for Lighter-weight Aircraft*, 2012: NASA/TM-2012-216008.

[4] Theodorsen, T., *General theory of aerodynamic instability and the mechanism of flutter*, in *Technical Report Archive & Image Library*1935, NACA: Unite state.

[5] Wright, J.R. and J.E. Cooper, *Introduction to aircraft aeroelasticity and loads*. Vol. 20. 2008, England: John Wiley & Sons. DOI: 10.1002/9781118700440

[6] Miles, J.W., *The aerodynamic force on an airfoil in a moving gust.* Journal of the Aeronautical Sciences, 1956. **23**(11): 1044-1050. DOI: 10.2514/8.3719

[7] Lomax, H., *Indicial aerodynamics*, in *AGARD Manual of Aeroelasticity,Part II,Chapter 6*1960, Advisory Group for Aeronautical Research and Development: United States.

[8] Singh, R. and J.D. Baeder, *Direct calculation of three-dimensional indicial lift response using computational fluid dynamics.* Journal of Aircraft, 1997. **34**(4): 465-471. DOI: 10.2514/2.2214

[9] Parameswaran, V. and J.D. Baeder, *Indicial aerodynamics in compressible flow-direct computational fluid dynamic calculations.* Journal of Aircraft, 1997. **34**(1): 131-133. DOI: 10.2514/2.2146

[10] Da Ronch, A., K.J. Badcock, Y. Wang, A. Wynn, and R. Palacios. *Nonlinear model reduction for flexible aircraft control design*. in *AIAA Atmospheric Flight Mechanics Conference*. 2012. Minneapolis, Minnesota. DOI: 10.2514/6.2012-4404

[11] Yang, G. and S. Obayashi, *Numerical analyses of discrete gust response for an aircraft.* Journal of Aircraft, 2004. **41**(6): 1353-1359. DOI: 10.2514/1.2531

[12] Raveh, D.E., *CFD-based models of aerodynamic gust response.* Journal of Aircraft, 2007. **44**(3): 888-897. 10.2514/1.25498

[13] Zhang, W., Z. Ye, Q. Yang, and A. Shi. *Gust response analysis using CFD based reduced order models*. in *47th AIAA Aerospace Sciences Meeting*. 2009. Orlando, Florida. DOI: 10.2514/6.2009-895

[14] Raveh, D.E. and A. Zaide, *Numerical simulation and reduced-order modeling of airfoil gust response.* AIAA journal, 2006. **44**(8): 1826-1834. DOI: 10.2514/1.16995

[15] Huang, R., H. Hu,Y. Zhao. *Nonlinear Reduced-Order Modeling for Multiple-Input/Multiple-Output Aerodynamic Systems. AIAA Journal*, 2014. 52(6): p. 1-13. DOI: 10.2514/1.J052323

[16] Huang, R., H. Li, H. Hu, and Zhao. *Open/Closed-Loop Aeroservoelastic Predictions via Nonlinear, Reduced-Order Aerodynamic Models. Aiaa Journal*, 2015. 53(7): p. 1-13. DOI: 10.2514/1.J053424

[17] Da Ronch, A., A. McCracken, K. Badcock, M. Widhalm, and M. Campobasso, *Linear frequency domain and harmonic balance predictions of dynamic derivatives.* Journal of Aircraft, 2013. **50**(3): 694-707. DOI: 10.2514/1.C031674

[18] Timme, S., K. Badcock, and A. Da Ronch. *Linear reduced order modelling for gust response analysis using the DLR-TAU code*. in *International Forum on Aeroelasticity and Structural Dynamics (IFASD)*. 2013. Bristol, U.K.

[19] Chen, G., J. Sun, and Y.M. Li, *Active flutter suppression control law design method based on balanced proper orthogonal decomposition reduced order model.* Nonlinear Dynamics, 2012. **70**(1): 1-12. DOI: 10.1007/s11071-012-0392-4

[20] Chen, G., X. Wang, and Y. Li, *A reduced-order-model-based multiple-in multiple-out gust alleviation control law design method in transonic flow.* Science China Technological Sciences, 2014. **57**(2): 368-378. DOI: 10.1007/s11431-013-5416-x

[21] Bartels, R. *Developing an accurate CFD based gust model for the truss braced wing aircraft*. in *31st AIAA Applied Aerodynamics Conference*. 2013. San Diego, CA. DOI: 10.2514/6.2013-3044

[22] Bekemeyer, P. and S. Timme. *Reduced order gust response simulation using computational fluid dynamics*. in *57th AIAA/ASCE/AHS/ASC Structures, Structural Dynamics, and Materials Conference*. 2016. San Diego, California. DOI: 10.2514/6.2016-1485

[23] Zhou, Q., G. Chen, A. Da Ronch, and Y. Li, *Reduced Order Unsteady Aerodynamic Model of a Rigid Aerofoil in Gust Encounters.* Aerospace Science and Technology, 2017. **63**: 203-213. DOI: 10.1016/j.ast.2016.12.029

[24] Van Leer, B., *Towards the ultimate conservative difference scheme. V. A second-order sequel to Godunov's method.* Journal of computational Physics, 1979. **32**(1): 101-136.

[25] Harder, R.L. and R.N. Desmarais, *Interpolation using surface splines.* Journal of Aircraft, 1972. **9**(2): 189-191. DOI: 10.2514/3.44330

[26] Yingtao, Z., L. Jingjing, C. Gang, L. Yueming, and G. Zhenghong. *Efficient Multidisciplinary Aerodynamic Optimization Design Based on Discrete Adjoint Method*. in *54th AIAA/ASME/ASCE/AHS/ASC Structures, Structural Dynamics, and Materials Conference*. 2013. Boston, Massachusetts. DOI: 10.2514/6.2013-1504

[27] Tsai, H., A. F. Wong, J. Cai, Y. Zhu, and F. Liu, *Unsteady flow calculations with a parallel multiblock moving mesh algorithm.* AIAA journal, 2001. **39**(6): 1021-1029. DOI: 10.2514/2.1442

[28] Zhou, Q., D. Li, A.D. Ronch, G. Chen, and Y. Li, *Computational fluid dynamics-based transonic flutter suppression with control delay*. Journal of Fluids & Structures, 2016. **66**: 183-206. DOI: 10.1016/j.jfluidstructs.2016.07.002

[29] Righi, M., M. Berci, M. Franciolini, A.D. Ronch, and D. Kharlamov. *Subsonic indicial aerodynamics for the unsteady loads of trapezoidal wings*. in *AIAA Aviation*. 2016. DOI: 10.2514/6.2016-4165

[30] Lesoinne, M., M. Sarkis, U. Hetmaniuk, and C. Farhat, *A linearized method for the frequency analysis of three-dimensional fluid/structure interaction problems in all flow regimes.* Computer Methods in Applied Mechanics and Engineering, 2001. **190**(24): 3121-3146. DOI: 10.1016/S0045-7825(00)00385-6

[31] Wang, S.-T. and W. Frost, *Atmospheric turbulence simulation techniques with application to flight analysis*, 1980, NASA CR-3309.

[32] Zhou, Q., G. Chen, Y. Li, and A.D. Ronch. *Aeroelastic Moving Gust Responses and Alleviation based on CFD*. in *AIAA Modeling and Simulation Technologies Conference*. 2016. DOI: 10.2514/6.2016-3837

[33] Yates Jr, E.C., *AGARD standard aeroelastic configurations for dynamic response I-wing 445.6*, in *Advisory group for aerospace research and development neuilly-sur-seine (FRANCE)*1988, DTIC Document.